NANO · MICRO small
www.small-journal.com

Macroscopic Carbon Nanotube Structures for Lithium Batteries

*Yufeng Luo, Ke Wang, Qunqing Li, Shoushan Fan, and Jiaping Wang**

Carbon nanotubes (CNTs) are regarded as one of the most promising materials to manufacture high-performance lithium batteries. This prospect is closely related to the construction of macroscopic architectures of CNTs. The superaligned CNT (SACNT) array is a unique kind of vertically aligned CNT array. Its highly oriented feature and strong intertube force facilitate the fabrication of macroscopic SACNT structures with various forms, including unidirectional films, buckypapers, and aerogels, etc. The as-produced SACNT macroscopic architectures are successfully introduced into lithium batteries due to their outstanding electrical and mechanical properties. Herein, an overview of the functions of macroscopic SACNTs in lithium batteries is proposed, including their applications in composite electrodes, current collectors, interlayers, and flexible full cells.

1. Introduction

Lithium batteries, including lithium-ion batteries (LIBs) and lithium metal batteries, are widely regarded as one of the most promising candidates for clean and renewable energy sources.[1–3] Lithium batteries have become an indispensable component for the information age, especially in serving as power sources for laptops, mobile phones, and other portable electronic devices. Moreover, lithium batteries are expected to be applied to other fields that have been powered by fossil fuels, such as electric vehicles and unmanned aerial vehicles, which will substantially address some crucial issues of energy shortage and environmental problems. Unfortunately, the promotion of lithium batteries is restricted by their limited performance, and one of the primary limitations comes from the energy densities. Generally, the state-of-the-art commercial lithium batteries exhibit energy densities less than 300 Wh kg^{-1}, which is a primary bottleneck for their uses in electric vehicles as it severely limits the endurance mileage.

There are several factors that affect the energy densities of lithium batteries. In addition to the development of active materials with high theoretical energy densities, the following requirements should be met for the charge–discharge processes. First, there should be sufficient conductive pathways for electron transfer, thus conducting agents, such as carbon blacks, are introduced. Second, the electrodes should possess high structural stability. The electrode integrity is provided by the polymer binder, which displays significant van der Waals force to combine the active materials and the conductive additives. Besides, metal current collectors support the electrode composites in order to improve their conductivity and ensure their mechanical robustness. These components do not contribute to electrode capacity directly, but they occupy quite a large proportion of the weight and volume of the lithium batteries.[4] Therefore, higher energy densities can be achieved by reducing these inert parts in the lithium batteries, and there are two approaches toward this target. One relies on searching lightweight alternatives, including current collectors and conducting agents with even higher electrical or mechanical properties; the other is optimizing the electrode structures.

Carbon nanotubes (CNTs) arouse attention among researchers because of their highly conductive and flexible nature. Moreover, their peculiar 1D morphology offers opportunities to fabricate different electrode structures. In fact, several efforts have been devoted to utilize CNTs as anode active materials due to their higher specific capacity than graphite. Unfortunately, these exertions have some insurmountable challenges, including the significant irreversible capacity and the lack of charge/discharge plateaus. By now, applying CNTs as auxiliary components, such as conductive agents and current collectors, is widely considered a more viable route to manufacture advanced lithium batteries. Nevertheless, there are still significant challenges when introducing CNTs in lithium batteries, as their outstanding properties can hardly be fully utilized in macroscopic structures. The large specific area of CNTs usually causes undesired agglomeration and tangled structures, which severely reduce the available surface area. Meanwhile, the agglomeration also introduces significant challenges on dispersion, structure control, and uniform mixture of CNTs and other components. In essence, the limitation of

Dr. Y. Luo, Prof. Q. Li, Prof. S. Fan, Prof. J. Wang
Department of Physics and Tsinghua-Foxconn
Nanotechnology Research Center
Tsinghua University
Beijing 100084, China
E-mail: jpwang@tsinghua.edu.cn
Dr. Y. Luo
School of Materials Science and Engineering
Tsinghua University
Beijing 100084, China
Dr. K. Wang
School of Materials Science and Technology
China University of Geosciences
Beijing 100083, China
The ORCID identification number(s) for the author(s) of this article can be found under https://doi.org/10.1002/smll.201902719.

DOI: 10.1002/smll.201902719

practical applications of CNTs stems from the difficulty in constructing macroscopic CNT architectures. One original idea is to synthesize CNTs with macroscopic tube length, but there still exist lots of unsolved technical problems.[5,6] Another route is to assemble nano- or microscaled CNTs into macroscopic structures, which usually requires sophisticated procedures. Superaligned CNTs (SACNTs) are well-oriented multiwalled CNT arrays that were first synthesized on silicon wafers by Fan and co-workers in 2002,[7] which can solve the problems mentioned above. **Figure 1**a and 1b show SEM images of ordinary vertically aligned CNT arrays and SACNT arrays,[8] respectively. It can be observed that there still exist a large amount of tangled structures in the ordinary arrays. The ordinary CNTs can hardly be dispersed and might even severely aggregate in composite electrodes, as illustrated in Figure 1c. On the contrary, the highly oriented nature of SACNTs effectively eliminates the undesired agglomerations. Meanwhile, there are fewer impurities and defects on the surfaces of SACNTs, which result in the strong van der Waals interaction among tubes.[9] It should be admitted that this strong intertube force can make adjacent nanotubes form bundles, which would incur difficulty on dispersion to some extent. But this difficulty can be effectively overcome with proper processing, which would be discussed later. Moreover, the strong van der Waals interaction, together with the well alignment, allows SACNTs to be end-to-end joined, forming various types of structures at macroscale. For instance, continuous films with unidirectional alignment can be easily obtained by pulling out SACNT bundles from the arrays, the length of which can reach 10^2 m level. Besides, continuous SACNT networks with random alignments, such as buckypaper and aerogel, are also available with proper dispersion of SACNTs. For the sake of clarity, "SACNT" in the following paragraphs refers to this special type of CNT array with well oriented feature and its derived macroscopic structures, even though some architectures are not "superaligned" any more after processing, such as buckpaper and aerogel. The subsequent discussion also involves some other forms of CNTs without highly oriented nature.

This article aims to provide an overview of the applications of macroscopic architectures based on SACNTs in lithium batteries developed in our group, as illustrated in **Figure 2**. The excellent conductivity and the convenience in dispersion make SACNTs competent to replace traditional conductive diluents, and better cell performance can be achieved with even fewer amounts of additives. Besides, SACNT-based architectures can simultaneously perform as structural scaffold due to the strong van der Waals force among tubes. The SACNT scaffold can effectively improve the strength and flexibility of the self-supporting composite electrodes without using any binder. The SACNT films with unidirectional alignment can also be cross-stacked to form an ultrathin and light membrane with high conductivity and strength. Such 2D structures facilitate to construct layer-by-layer composite electrodes and also show great promise for use as current collectors and functional interlayers. Moreover, considering the distinctions between half-cell and full-cell tests, this review also illustrates some works about flexible full cells containing SACNTs, in order to further evaluate the macroscopic structures under the conditions in commercial batteries.

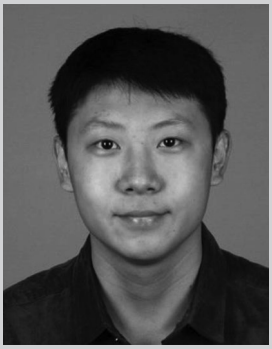

Yufeng Luo is a research associate at the Hong Kong Polytechnic University. He received a bachelor's degree in materials science and engineering from Jilin University in 2014 and a Ph.D. degree in materials science and engineering from Tsinghua University in 2019. His research is focused on the design, synthesis, and applications of nanomaterials for lithium batteries.

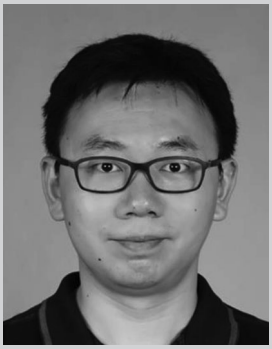

Ke Wang is a lecturer in the Department of Materials Science and Technology at China University of Geosciences, Beijing. He received a bachelor's degree in materials science and engineering from Tsinghua University in 2010 and a Ph.D. degree in physics from Tsinghua University in 2015. His research interests include the design and synthesis of electrode materials, and nanomaterials for lithium-ion batteries and metal–air batteries.

Jiaping Wang is a Professor in the Department of Physics at Tsinghua University. She received a bachelor's degree in materials science and engineering from Tsinghua University in 1996 and a Ph.D. degree in materials science from the University of Cambridge in 2002. She worked as an assistant professor at Louisiana State University before joining Tsinghua University in 2007. Her research focuses on the fabrication, properties, and applications of functional nanocomposite materials and devices.

2. Applications of Macroscopic SACNT Structures in Composite Electrodes

2.1. SACNT/$LiCoO_2$ Composite Cathodes

$LiCoO_2$ is the most commonly used cathode material in the state-of-the-art LIBs. Many works have been carried out to fabricate high-performance composite cathodes with single- and multiwalled CNTs.[10–14] CNTs were utilized to compensate

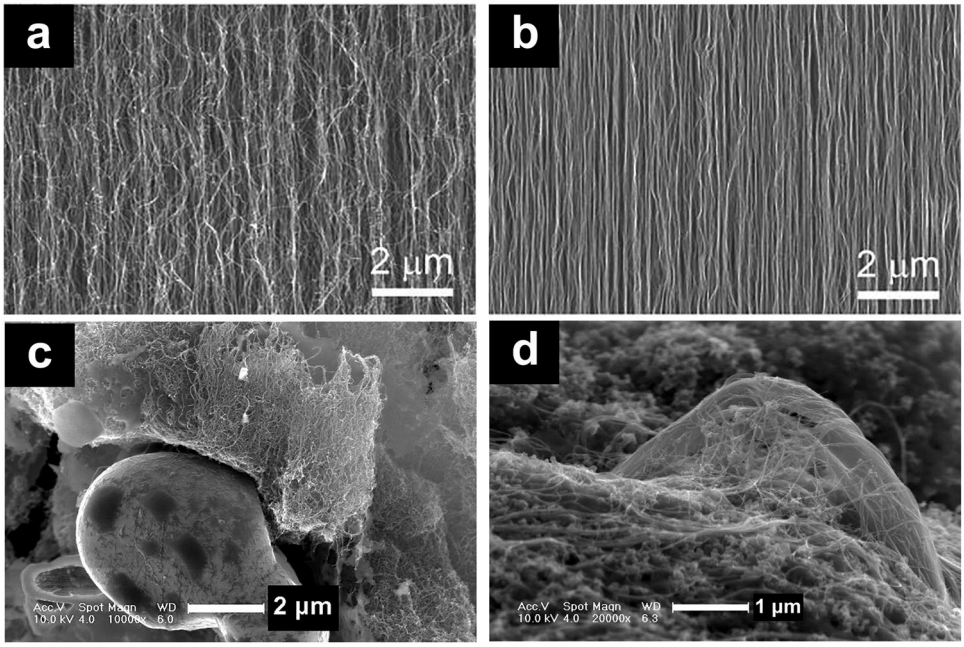

Figure 1. SEM images of a) ordinary vertically aligned CNT arrays and b) SACNT arrays. Morphology of the composite cathodes fabricated by mixing c) ordinary CNTs and d) SACNTs with $LiCoO_2$ powders. Reproduced with permission.[8] Copyright 2008, American Chemical Society.

for the low conductivity nature of $LiCoO_2$ (10^{-3} S cm^{-1}) and its alternatives, such as $LiMn_2O_4$ (10^{-4} S cm^{-1}) and $LiFePO_4$ (10^{-9} S cm^{-1}).[15–17] In comparison to conventional conductive additives, i.e., carbon black, the much higher conductivity and larger aspect ratio of CNTs show superiority in reducing the percolation threshold. In other words, the proportion of conductive additives can be reduced. The dispersion of CNTs should also be considered. CNT agglomerations

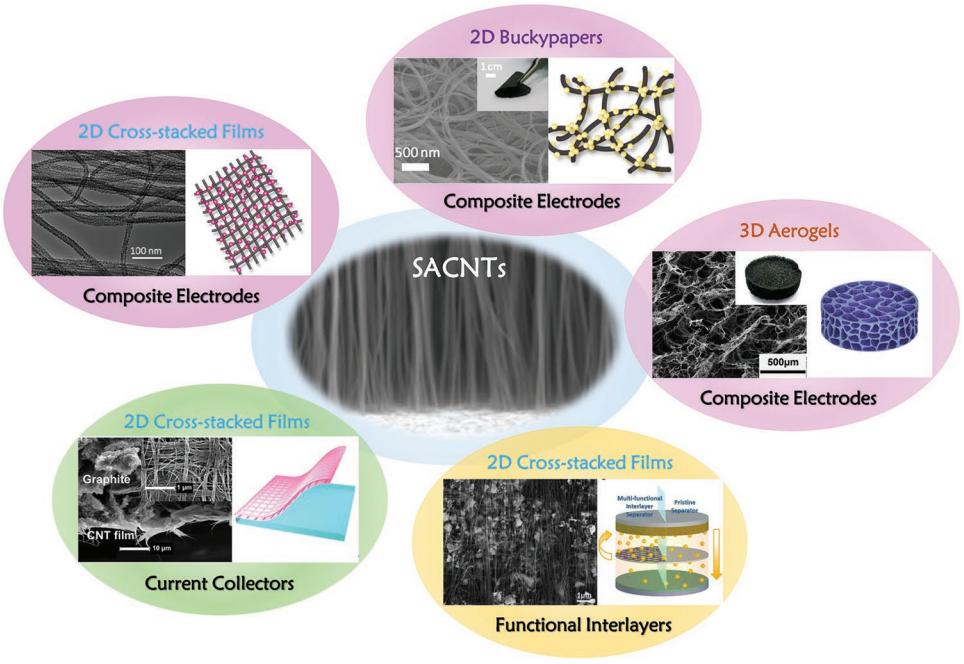

Figure 2. Illustration of applications of various macroscopic SACNT architectures (highly oriented films, buckypapers, and aerogels) in different components of lithium batteries, including composite electrodes,[27,37,39] current collectors,[50] and functional interlayers.[56] Adapted with permission.[9] Copyright 2011, Wiley-VCH. Adapted with permission.[27] Copyright 2016, American Chemical Society. Adapted with permission.[37] Copyright 2013, American Chemical Society. Adapted with permission.[40] Copyright 2018, American Chemical Society. Adapted with permission.[50] Copyright 2013, Wiley-VCH. Adapted with permission.[56] Copyright 2017, Wiley-VCH.

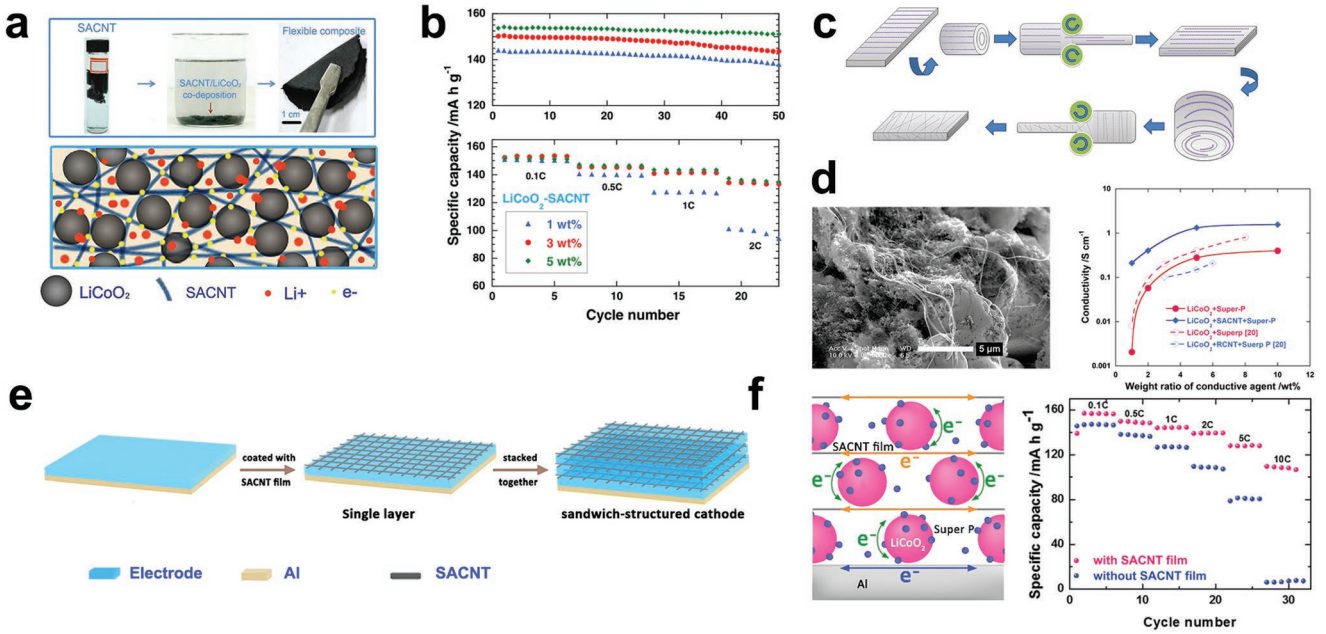

Figure 3. a) Fabrication of the binder-free $LiCoO_2$–SACNT composite electrodes by ultrasonication and codeposition and schematic of its structural configuration. b) Cycle and rate performance of the binder-free $LiCoO_2$–CNT composite electrodes. Reproduced with permission.[18] Copyright 2012, Wiley-VCH. c) Schematic of the cold-rolling procedure to fabricate $LiCoO_2$–SACNT–Super P composites. d) SEM image of the CNT–Super P hybrid conductive network and the comparison in electrical conductivities of the $LiCoO_2$–Super P, $LiCoO_2$–SACNT–Super P, and $LiCoO_2$–RCNT–Super P electrodes. Reproduced with permission.[19,20] Copyright 2013 and 2010, Elsevier, Inc. e) Schematic of the fabrication procedure for sandwich-structured cathodes with SACNT conductive layers. f) Schematic of the layer-by-layer cathode structure and the rate performance of the $LiCoO_2$–2 wt% Super P cathode with and without SACNT conductive layers. Reproduced with permission.[21] Copyright 2017, The Royal Society of Chemistry.

should be limited to avoid the polarization due to the uneven dispersion of CNTs.

As aforesaid, SACNTs possess the "superaligned" nature, which is an excellent merit to mix the active materials and SACNTs homogeneously in a controlled structure. Besides, the high conductivity and strong van der Waals interaction make SACNTs serve as multifunctional components, which provide not only electron pathways, but also structural framework. A binder-free $LiCoO_2$–SACNT cathode was fabricated through a facile ultrasonication and codeposition technique, as shown in **Figure 3**a.[18] During ultrasonication, the SACNT arrays could be sufficiently dispersed in the organic solvent, expanding into a continuous 3D network with a volumetric increase of more than 100 times. After the evaporation of ethanol, binder-free and flexible $LiCoO_2$–SACNT cathodes were obtained, and the $LiCoO_2$ microparticles were homogeneously dispersed in the SACNT conductive network. As shown in Figure 3b, the $LiCoO_2$–3 wt% SACNT electrode displayed a reversible specific discharge capacity of 151.4 mAh g^{-1} at 0.1 C after 50 cycles and a high specific capacity of more than 130 mAh g^{-1} at 2 C. The excellent electrochemical performance reflects the advantages of the continuous SACNT network, where electrons can rapidly migrate along the SACNTs, and lithium ions can quickly get access to the active materials through the porous structure. Besides, the robust structural framework with high flexibility can endure volumetric change during charge and discharge. To further reduce the use of the SACNTs and make them more economically viable for commercial electrodes, a hybrid conductive network consisting of SACNTs and Super P was designed.[19] As shown in Figure 3c,d, 20 layers of SACNT films were combined with $LiCoO_2$–Super P-PTFE composites through a facile cold-rolling procedure, and highly homogeneous mixture of all these components was achieved. The weight ratio of SACNTs in the $LiCoO_2$–SACNT–Super P composite was less than 0.01%, which was almost negligible. The small amount of SACNTs was adequate to form long-range conductive pathways throughout the composite, showing a conductivity increase of two orders of magnitude in the $LiCoO_2$–SACNT-1 wt% Super P composites (from 2.06×10^{-3} to 2.72×10^{-1} S cm^{-1}, as shown in Figure 3d). Super P in the hybrid conductive additive could provide short-range conductive pathways along the surface of $LiCoO_2$ particles, and rapid reaction kinetics was realized. Galvanostatic charge–discharge test demonstrated that $LiCoO_2$ electrodes with the hybrid SACNT–Super P conductive network exhibited excellent cycle stability (150 mAh g^{-1} at 0.1 C with a capacity retention of 99.7% after 50 cycles) and decent rate capability (87 mAh g^{-1} at 5 C). The conductivity of the $LiCoO_2$–SACNT–Super P cathodes is also compared with the electrodes containing ordinary multiwalled CNTs. Park et al. combined random-oriented CNT (denoted as RCNT in Figure 3d) with $LiCoO_2$ and Super P using an ultrasonic method.[20] The conductivity decreased when Super P was replaced with RCNT, due to the poor distribution of RCNTs in electrodes.

Apart from randomly oriented SACNT networks, unidirectional SACNT films can also help to construct high-performance $LiCoO_2$ composite cathodes. As shown in Figure 3e, a sandwich-structured $LiCoO_2$–Super P-SACNT electrode was

fabricated by repeating the procedures of casting slurry and cross-stacking SACNT films alternatively.[21] Only two layers of cross-stacked SACNT films were adequate to perform as an efficient conducting layer within the cathode, resulting in a conductivity increase of one order of magnitude in the $LiCoO_2$–2 wt% Super P composite (from 1×10^{-3} to 3.1×10^{-2} S cm^{-1}). Meanwhile, such SACNT conducting layer weighted no more than 0.04% in the electrode. More importantly, almost all $LiCoO_2$ particles, regardless of the thickness of the electrode, were able to contact the SACNT conducting layers in this layer-by-layer construction (Figure 3f). The microstructure of the electrodes ensured that electron transportation would not be deteriorated in thicker electrodes. As a consequence, polarization can be prohibited even when more active materials were loaded by increasing the number of $LiCoO_2$ and conductive layers, and therefore, excellent electrochemical performance can be achieved in thicker cathodes. With a thickness comparable to commercial LIBs, this sandwich-structured $LiCoO_2$–2 wt% Super P-SACNT cathode still exhibited an impressive specific capacity as high as 109.6 mAh g^{-1} at 10 C (Figure 3f), which is one of the best rate capabilities reported so far for commercial microsized $LiCoO_2$ powders.

In sum, SACNT can be introduced into $LiCoO_2$ composites with various forms, including random-oriented network and unidirectional films. In comparison with ordinary CNTs, SACNTs are more favorable for a uniform dispersion. All these SACNT/$LiCoO_2$ composites displayed significant improvement in conductivity and cell performance, indicating that SACNTs have been sufficiently utilized.

2.2. SACNT/S Composite Cathodes

Li–S battery, as a promising candidate for next-generation high-density energy storage devices, has attracted intense interests among researchers during the last decade due to its high theoretical specific capacity and energy capacity of 1675 mAh g^{-1} and 2600 Wh kg^{-1}.[22] Besides, the abundance and non-toxicity of sulfur make Li–S battery more environmentally friendly. Different from other commercial "intercalation reaction" cathodes in Li-ion batteries, such as $LiCoO_2$ and $LiFePO_4$, element sulfur, with a two-electron reaction, is a typical cathode material based on "conversion reaction." The electrochemical reaction of S cathodes is restricted by their low intrinsic conductivity and significant volumetric changes during cycling. Besides, other significant drawbacks also hinder the practical application of Li–S batteries. During the discharge process, a series of intermediates of polysulfides, which are soluble in the ether organic electrolyte, form through the cleavage of the S-S bond in cyclo-S8 and the combination of Li ions. These dissolved intermediates can "shuttle" between cathodes and anodes, resulting in poorly controlled electrode–electrolyte interface and fast capacity fading. How to inhibit the "shuttle effect" has become the main challenge of Li–S batteries.

Making sulfur–carbon composites with carbonaceous matrix, such as graphene, CNTs, and carbon nanofibers, has proved to be an effective method to tackle the issues mentioned above. The high specific surface areas of these carbonaceous materials can provide vast anchoring sites for sulfur, and the high conductivity and excellent wettability for ether electrolytes can facilitate sufficient electron transfer and lithium ion diffusion to compensate for the sluggish kinetics in the electrochemical reaction. As illustrated in Section 2.1, SACNT arrays can construct 3D macroscopic conductive networks in ethanol solution by ultrasonication, which works as the matrix in binder-free electrodes. This method is also applicable to the fabrication of binder-free nano S-SACNT composite,[23] as shown in **Figure 4**a. The SACNT network provides sufficient porosity and continuous electron pathways. High porosity can promote the infiltration of the electrolyte due to its lipophilicity and alleviate the collapse of the microstructure resulted from the volume expansion/shrinkage during cycling. Benefited from these advantages, nano S-SACNT composite cathodes exhibited excellent cycling and rate performance. After 100 cycles at 1 C, the battery delivered a reversible capacity of 909 mAh g^{-1} with a capacity retention of 85%. Even at 10 C, it displayed an

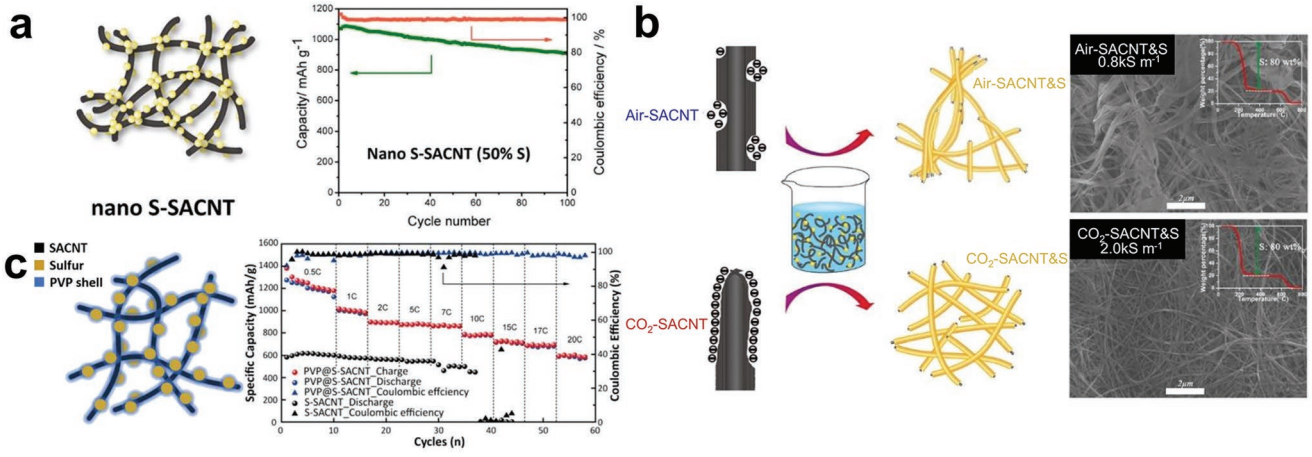

Figure 4. a) Schematic of the synthesis procedure of nano S-SACNT composite and its cyclic performance. Reproduced with permission.[23] Copyright 2014, American Chemical Society. b) Schematic of the synthesis procedure and SEM images of the air-CNT&S and CO_2–CNT&S composites. Reproduced with permission.[28] Copyright 2018, Elsevier, Inc. c) Schematic of the synthesis procedure of PVP@S-CNT composite and its rate performance. Reproduced with permission.[30] Copyright 2016, Elsevier, Inc.

impressive capacity of 879 mAh g^{-1}. Introducing graphene nanosheets into the S-SACNT system could add another physical barrier to constrain sulfur, and the S-SACNT/graphene cathodes demonstrated superior long-term cycling stability over 1000 cycles at 1 C, with a capacity fade as low as 0.041% per cycle.[24]

Although confining sulfur in the carbonaceous nanostructures is an effective method to promote the electrochemical reactions, including the reduction of sulfur and oxidation of Li_2S, it was challenging to completely trap polysulfides just based on the physical adsorption due to the nonpolar surface of carbonaceous materials. The polysulfides could still dissolve into the electrolyte once they were solvated. Heteroatom doping has been investigated as an efficient way to change the surface-polarity of carbonaceous materials. Both density functional theory (DFT) simulation and experimental results have demonstrated that heteroatom-doping can effectively improve the electrochemical performance of Li–S batteries by trapping polysulfides and facilitating the decomposition of Li_2S.[25] According to the DFT results, introducing N and O atoms into carbonaceous materials is the most effective way to enhance their chemisorption with polysulfides through the dipole–dipole electrostatic interactions.[26] Therefore, based on the configuration of binder-free nano S-SACNT electrodes, heteroatom doping was carried out to improve the confinement of polysulfides. O atoms were successfully introduced into SACNTs through controlled oxidation in the air,[27] which is denoted as air-SACNTs. Also, mesopores were introduced onto the surface of SACNTs by heat treatment at 550 °C. The mesopores provided additional sites for sulfur loading, especially when the content of sulfur exceeded 50 wt%. The air-SACNT&S composites exhibited excellent electrochemical performance with a 70% sulfur loading. At 0.1 C, the composite cathode delivered a reversible capacity of 528 mAh g^{-1} based on the whole weight of electrode after 100 cycles. However, bundles of SACNTs still cannot be fully untied by the oxidation in the air so that the surfaces of SACNTs cannot be utilized efficiently, especially for the higher sulfur loading cathodes. Thus, a milder and more uniform oxidation method was proposed by using carbon dioxide (CO_2).[28] After introducing the functional groups containing O atoms, negative charges can be carried on the external surface of SACNTs (Figure 4b), so that the treated SACNTs had lower Zeta potential. Therefore, electrostatic repulsive forces made the dispersal of SACNTs more stable and efficient, and even higher sulfur loading was realized. The CO_2–SACNT&S electrode with 80 wt% sulfur loading exhibited a reversible capacity of 430.5 mAh g^{-1} after 300 cycles at 0.2 C, with a low fade rate of 0.172% per cycle.

Similar to heteroatom doping, conductive polymers, such as poly(3,4-ethylene dioxythiophene), polyaniline, and polyvinyl pyrrolidone (PVP), also contain functional groups that have strong chemisorption to the polysulfides to suppress the "shuttle effect."[29] PVP@S-SACNT composite electrode was prepared by a simple solution-based method (Figure 4c).[30] PVP not only helps to disperse the SACNTs but also provides an outer shell to capsule the nano S particles. The obtained composite cathode showed an excellent rate performance and delivered a discharge capacity of 590 mAh g^{-1} at 20 C.

2.3. SACNT Composite Anodes

Artificial and natural graphites are the most popular anode materials for LIBs. However, their performance can hardly satisfy the demand for future lithium batteries, especially for power batteries in electric vehicles. The low theoretically specific capacity of graphite (≈372 mAh g^{-1}) cannot meet the requirement for longer endurance mileage. Some additives, such as SiO_x, have been introduced into the electrodes to enhance their energy densities and reaction stability.[31] Besides, research was carried out to seek alternative anode materials for higher energy densities and improved safety. Spinal-phase $Li_4Ti_5O_{12}$ (LTO) is a very promising anode because of its stable operating voltage, fast lithium ion mobility, and excellent structural stability during cycling, which are beneficial to address the safety issues. However, the low conductivity limits its practical application.[32] A simple solution-based method was performed to prepare a mesoporous LTO composite anode with SACNTs (**Figure 5**a).[33] Dissolved in H_2O–ethanol dispersion of SACNTs, followed by heat treatment at 400 °C, mesoporous LTO nanoclusters were in situ synthesized in a 3D continuous SACNT network (denoted as LTO@SACNT-400). Neither binder nor current collector was needed. Like the binder-free cathodes demonstrated above, the SACNT networks act as efficient conductive pathways and robust mechanical skeleton, and sufficient electron transport and lithium ion diffusion are guaranteed. The LTO@SACNT-400 showed an outstanding rate performance with a capacity of 164.3 mAh g^{-1} at 20 C, as well as a reversible capacity of 165.5 mAh g^{-1} after 400 cycles at 1 C, reflecting a stable cycling performance with a nearly 95.3% retention.

Another attractive anode material is based on transition metal oxides (TMOs). According to the different reaction mechanisms, TMOs can be divided into two types:[34] (1) intercalation–deintercalation mechanism: lithium ions insert and desert in the layered crystalline structure during cycling without the formation of Li_2O, such as WO_2 and T-Nb_2O_5; (2) conversion mechanism: TMOs undergo redox reaction with lithium during cycling, accompanied by the formation of Li_2O and transition metal (TM) such as Co_3O_4, Fe_3O_4, and MnO_2. TMOs based on intercalation–deintercalation mechanism possess outstanding cycling performance, flat charge/discharge plateau, and tiny volumetric expansion, but comparatively low theoretical specific capacity and higher working potential. For the TMOs materials based on conversion mechanism, their higher specific capacities are accompanied with more massive volumetric expansion. Besides, low conductivity and initial coulombic efficiency severely affect their electrochemical performance. Through thermal decomposition, sol–gel, and physical vapor deposition methods, a series of binder-free TMO/SACNT composite electrodes (Mn_3O_4, Co_3O_4, Fe_3O_4, MnO_2, and TiO_2) were successfully prepared, based on the 2D macroscopic architecture of SACNTs (Figure 5b–d).[35–39] By regulating experimental parameters, such as precursor concentration and reaction time, all these composite electrodes showed remarkable mechanical properties and electrochemical performance, especially the rate performance, which profited from the high conductivity of SACNTs. By combining the continuous dry-drawn SACNT film technique and the magnetron sputtering method, a one-step

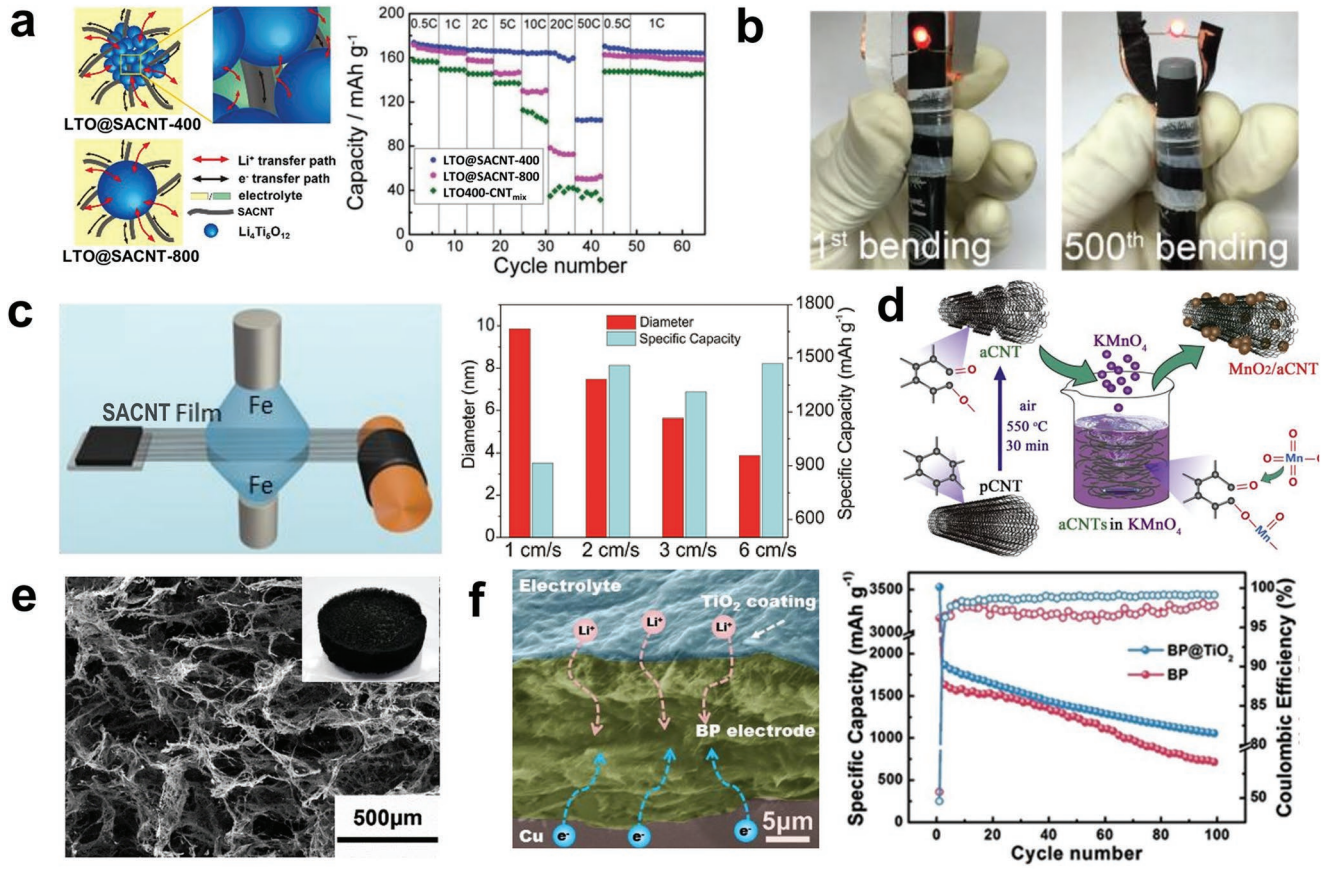

Figure 5. a) Illustration of the electron and lithium ion transfer paths in LTO@SACNT electrodes and its corresponding rate performance. Reproduced with permission.[33] Copyright 2016, The Royal Society of Chemistry. b) Optical photographs of an SACNT buckypaper-based electrode lighting an LED in a bent state. Reproduced with permission.[39] Copyright 2018, American Chemical Society. c) Schematic of the synthesis of Fe_3O_4–SACNT composites by magnetron sputtering and the comparison of the average particle diameter and the discharge capacity at different SACNT film drawing speeds. Reproduced with permission.[37] Copyright 2013, American Chemical Society. d) Schematic of the fabrication process of MnO_2/aCNT composites. Reproduced with permission.[38] Copyright 2018, Elsevier, Inc. e) SEM and optical images of a 3D SACNT-aerogel-based electrode. Reproduced with permission.[40] Copyright 2018, American Chemical Society. f) SEM image of the cross-section of a BP@TiO_2 electrode and its cyclic performance. Reproduced with permission.[42] Copyright 2018, American Chemical Society.

synthetic approach was developed to obtain Fe_3O_4–SACNT composite electrodes (Figure 5c). The Fe_3O_4–SACNT electrode delivered a reversible capacity over 800 mAh g^{-1} at a current density of 0.1 A g^{-1} based on the total mass of the electrode.[37] Through in-situ redox reaction of $KMnO_4$ and air-oxidized SACNTs (aCNTs), MnO_2/aCNT electrodes were fabricated and showed capacitive characteristics, which provided the basis for ultrafast lithium storage (Figure 5d).[38]

SACNTs can also easily self-assemble into macroscopic 3D aerogels via a simple ultrasonication and freeze-drying procedure, without using any organic binder or templates. The SACNT aerogel exhibits high "honeycomb-like" porosity and large specific surface area, which are great advantages to accommodate TMO electrodes. A series of high-loading TMO/SACNT electrodes (5 mg cm^{-2}) based on the SACNT aerogel were prepared, including MnO_2, NiO, Fe_2O_3, and Co_3O_4, through a facile freeze-drying and calcination process (Figure 5e).[40] The highly conductive 3D SACNT aerogel provides efficient electron pathways, and their good wettability to the carbonate electrolyte and high porosity can shorten the distance of lithium ion diffusion. Besides, a TM–O–C linkage formed during the synthesis process, and the composite electrodes exhibited excellent cycling and rate performance.

Black phosphorus (BP), as a typical 2D material, has attracted widespread attention due to its unique characteristics. Its high theoretical specific capacity (≈2596 mAh g^{-1}), large gap between adjacent phosphorene, and fast lithium ion diffusion along the zigzag direction make BP a promising anode material for LIBs.[41] Similar to other anode materials based on alloying reaction, such as silicon and tin, BP suffers fast capacity fading due to the significant volumetric expansion (≈300%) and the propagation of the solid electrolyte interlayer. Moreover, the final lithiation product, Li_3P, is insulating and electrochemically inactive. A large amount of conductive additives is required, sometimes even more than 50 wt%. To solve these problems, truncated SACNTs were used as conducting agents to reduce its percolation threshold effectively and enhance the electrochemical performance of the BP anode (Figure 5f).[42] Even though many voids and macropores were generated during cycling owing to the severe expansion/shrinkage of the BP particles,

SACNTs bridged different parts of the electrode to maintain a conducting network. To further improve the performance of the BP electrode, a nano-TiO_2 coating was performed onto the electrode surface. The BP@TiO_2 electrode showed a 48% capacity increase and smaller polarization compared to the bare BP electrode.

3. Current Collectors Using SACNT Films

Generally, electrodes in commercial LIBs are not freestanding and need to attach on metal foils, i.e., the current collectors, which not only provide mechanical support for the electrodes but also electrically connect with lead. Considering electrochemical stability, the positive electrodes usually stick on Al foils, while the negative ones stick on Cu foils. Both kinds of metal foils are suitable for present LIBs, ascribed to their mechanical robustness, high conductivity, and acceptable cost. However, the main limitation of metal current collectors arises from their heavyweights. Al foils occupy about 15 wt% of the total mass of cathode, while Cu foils even account for as high as 50 wt% in the anode.[4] Besides, the adhesion between the electrode and the metal foil is not firm enough, and there is a relatively high probability of generating gaps at the interface with volumetric variations during cycling. The microfractures weaken the electrical connection between the electrode and current collector and lead to a capacity loss. The corrosion issue during electrochemical reaction should also not be ignored, such as the localized pitting corrosion in Al and the environment assisted cracking in Cu.

In order to find alternatives for metal current collectors with lighter weight and higher electrochemical stability, several attempts have been carried out using carbonaceous materials, such as graphene, CNTs, and carbon fibers.[43–49] Generally, the carbonaceous current collectors can be obtained from liquid dispersion followed by filtration or precipitation. This process usually generates disordered microstructure with a lot of small cavities and voids, which might result in a loose packing and comparatively large thickness. Even though these carbonaceous current collectors provide a practical route to increase the gravimetric energy densities, their improvement in volumetric energy densities is always limited. Some carbonaceous current collectors are even thicker than the metal foils,[47,49] which would undoubtedly sacrifice the volumetric energy densities.

In essence, the improvement of volumetric energy densities depends on the controlling of nano-/micropacking pattern, on which SACNTs own significant superiority. On one hand, the extremely low degree of disorder in SACNT arrays effectively avoids tangled structures at nano-/microscale, which is one main resource for the loose packing. On the other hand, the alignment of SACNTs can be easily adjusted by drawing them into unidirectional films, which is beneficial to increase packing density. In fact, one novel current collector with ultralightweight and small thickness has been fabricated by cross-staking 20-layer SACNT films (**Figure 6**a).[50] The areal density of this SACNT current collector is only 0.04 mg cm^{-2}, accounting for no more than 1 wt% of typical Al and Cu current collectors. Meanwhile, the thickness of the current collector could be less than 1 µm. As a result, the energy densities, based on the overall weight and volume of electrodes, would be significantly improved. In comparison to the graphite–Cu electrode, the graphite–SACNT electrode with a thickness of 88 µm, demonstrated more than 180% and 30% improvements in gravimetric and volumetric energy densities. Moreover, the SACNT current collectors possess superior interfacial property. The SACNT films show a smaller contact angle and better wettability to the electrode slurry than metal foils (Figure 6b). Thus, the intimate connection would be realized when casting slurries on the SACNT current collectors. The crossed patterns of SACNT current collectors generated porous morphology with a much

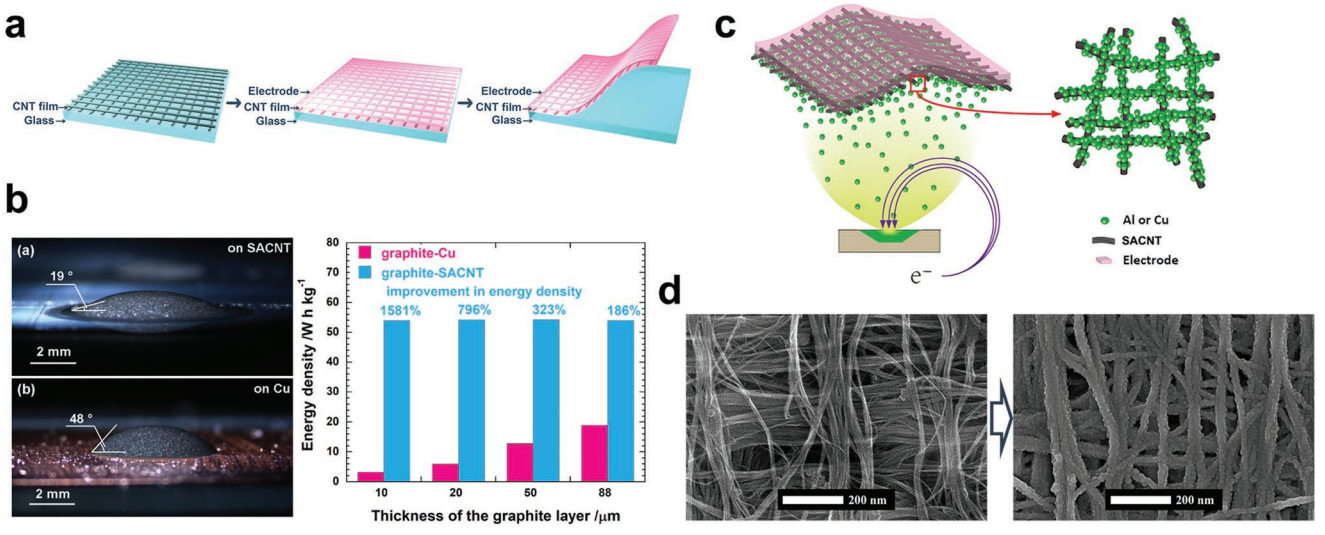

Figure 6. a) Schematic of the procedure for fabricating electrodes with SACNT current collectors. b) Comparison of wettability and gravimetric energy densities between SACNT and Cu current collectors. Reproduced with permission.[50] Copyright 2013, Wiley-VCH. c) Schematic of the surface modification of SACNT current collectors by electron-beam evaporation. d) SEM images of the morphology of a CNT current collector before and after modification. Reproduced with permission.[51] Copyright 2017, Elsevier, Inc.

larger contact area. Accordingly, stronger adhesion and lower contact resistance were realized, leading to smaller polarization, better cycle stability, and high rate performance. The graphite–SACNT electrode delivered a specific capacity of 335 mAh g^{-1} at 0.1 C, with a capacity retention of 99.1% after 50 cycles. At 2 C, the specific capacity was still as high as 326 mAh g^{-1}.

Even though the novel SACNT current collectors exhibits great potential to realize higher energy density, their the relatively poor macroscopic conductivity still needs to be improved in order to fabricate large-size electrodes. For example, a 20-layer cross-stacked SACNT film delivers a sheet resistance of more than 100 Ω sq^{-1}, which will generate noticeable polarization in the scaled-up electrodes, especially along the lateral direction. Fortunately, this drawback can be effectively relieved by coating a thin metal film (Figure 6c,d).[51] After thin-coating of Al or Cu by electron-beam evaporation, the sheet resistance of the SACNT current collector was lowered by three orders of magnitude (≈0.3 Ω sq^{-1}). The intimate connection at the electrode–SACNT interface was not affected, as the metal film deposited on the other side of the SACNT current collector. Meanwhile, the coating layer led to very little increase in mass and volume, both of which did not exceed 1 wt% of the corresponding electrodes. Though the weight and volume of the electrode were slightly increased, the polarization was well limited, and the energy densities were improved eventually.

Generally speaking, the SACNT films are distinguished from metal foils by their much smaller weight and thickness, as well as the stable connection with electrodes. In addition, both SACNT films and metal foil current collectors share similar procedures for fabricating electrodes. Therefore, the SACNT current collectors should display high compatibility with commercial LIBs. **Table 1** shows micromorphology and areal densities of current collectors based on SACNTs and ordinary CNTs that reported in the literature.[45–47,50,51] Even though in some work, CNT current collectors were fabricated with quite small thickness (less than 5 μm), their areal density was usually larger by at least one order of magnitude than that of the SACNT current collectors. Such comparison indicates that proper tuning of the micromorphology does help to utilize the carbon nanomaterial more sufficiently. Besides, current collectors based on ordinary CNTs are usually fabricated through filtration or precipitation, thus their areas are often limited by the sizes of containers. In comparison, the length of continuous SACNT films can reach 10^2 m, which possesses larger potential for fabricating large-size electrodes.

Table 1. Micromorphology and areal densities of current collectors using SACNTs and ordinary CNTs.

Categories of current collector	Orientation of CNT	Thickness [μm]	Areal density [mg cm^{-2}]
SACNT[50]	Cross-stacking	<1	0.04
200 nm Al coating on SACNT[51]	Cross-stacking	<1	0.08
200 nm Cu coating on SACNT[51]	Cross-stacking	<1	0.18
CNT thin film[45]	Random	≈2	≈0.2
CNT fabric[46]	Random	3–5	<0.3
CNT tissue with double electro-coated Cu[47]	Random	5–6	2–2.2

4. Functional Interlayers Based on SACNT Films

Separator is a crucial component in the battery system, which is used to prevent the short circuit between cathode and anode. Functional modification to the separator is an effective method to stabilize the surface of the electrode, especially for Li–S batteries.[52] Many efforts have been made to suppress the migration of polysulfides by introducing an interlayer between sulfur cathode and separator. Most of the interlayers are based on carbonaceous materials, which benefited from their high conductivity that can provide extra electron pathways to reduce the polarization of the electrode. Besides, carbonaceous materials can provide more sites to capsule the solvated polysulfides. Therefore, this strategy has been an effective way to improve the electrochemical performance of Li–S batteries.

An ultrathin SACNT interlayer was prepared by cross-stacking 100 layers of SACNT films (**Figure 7**a),[53] and the rate capability of the sulfur electrode composed of sulfur powder, Super P, and PVDF was significantly increased. The cell performance of the pristine cathode with a sulfur loading of 50 wt% was quite poor, and it almost failed to display any capacity at current rates higher than 1.5 C. Contrarily, cathode with the SACNT interlayer could still keep a capacity more than 700 mAh g^{-1} at 3 C, even with a higher sulfur loading (60 wt%).

As mentioned in Section 2.2, nonpolar characteristics of carbonaceous materials limit the chemisorption capacity for the polysulfides. Some polar inorganics, such as transition metal oxides, sulfides, nitrides, and carbides, have been introduced into the Li–S battery system to suppress the "shuttle effect" by adsorbing polysulfides.[54] Moreover, some inorganics can play a catalytic role in the conversion of polysulfides and lithium sulfides during cycling, which can further improve the capacity and coulombic efficiency. An interlayer consisting of MoS_2 nanosheets and SACNT films was introduced at the interface between cathode and separator to improve the electrochemical performance (Figure 7b).[55] The pristine S cathode with the MoS_2/SACNT interlayer showed a reversible capacity of 770 mAh g^{-1} at 0.2 C after 200 cycles. Even at 10 C, the discharge capacity remained 784 mAh g^{-1}. The corrosion of lithium surface and the self-discharge problems were effectively suppressed. MoP_2, as a commercial catalyst for hydrogen evolution reaction, was also utilized to improve the energy densities of Li–S batteries.[56] To verify the electrocatalytic effects of the inorganic additives, a transparent pouch cell was designed to perform an in situ Raman test. The results of Raman spectra from both sides of the electrodes with different interlayers at 2.08 V demonstrated that the SACNT films physically hindered the polysulfides migration. Meanwhile, from the cathode side, the reaction products of the battery with the MoP_2/SACNT interlayer at 2.08 V were Li_2S_4 and Li_2S_2, while the products with the pristine separator were Li_2S_6 and Li_2S_2. These results suggest that the MoP_2 nanoparticles can accelerate the conversion of the polysulfides (Figure 7c).

Combining the unique characteristics of the SACNT films and graphene oxides,

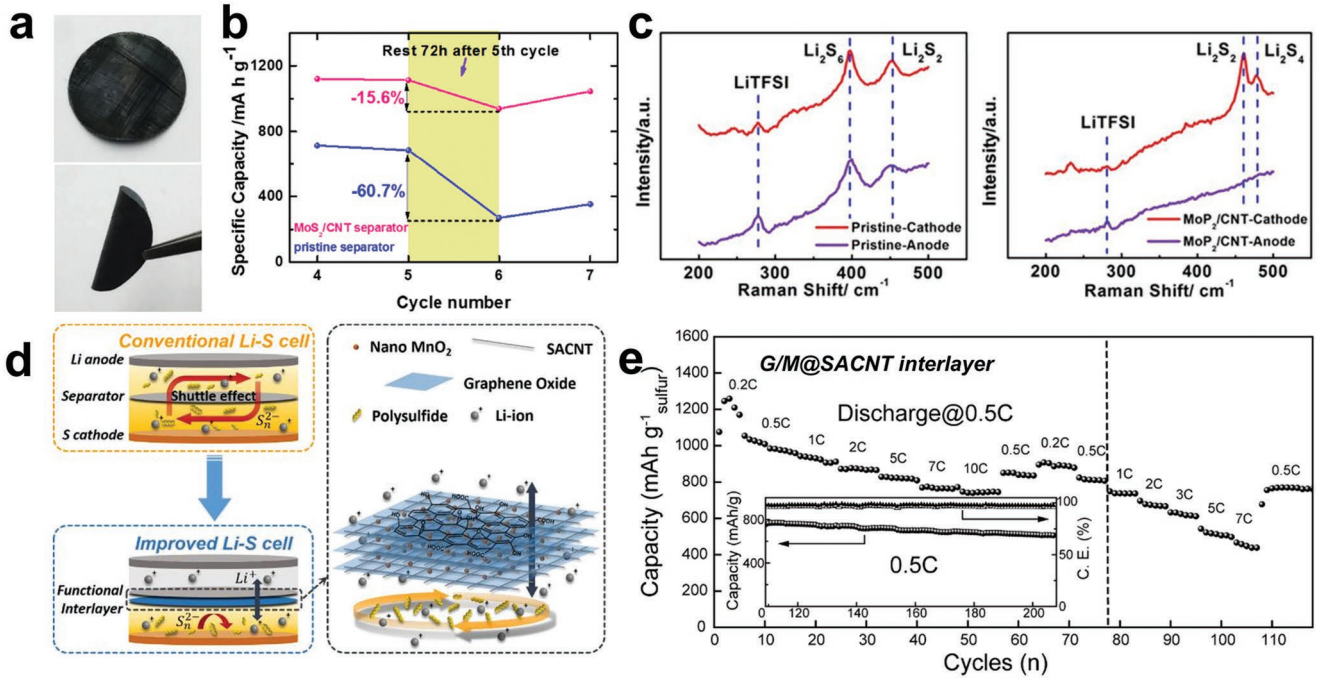

Figure 7. a) Optical photographs of the SACNT functional interlayer. b) Self-discharge behavior of the electrodes with the MoS_2/SACNT-interlayer-coated separator and the pristine separator. Reproduced with permission.[55] Copyright 2018, Elsevier, Inc. c) Raman spectra of the Li–S cell with the pristine separator and the CNT/MoP_2 interlayer at 2.08 V. Reproduced with permission.[56] Copyright 2017, Wiley-VCH. d) Schematic and e) rate performances of the electrode with the functional G/M@SACNT interlayer. Reproduced with permission.[57] Copyright 2017, Wiley-VCH.

an ultrathin MnO_2/graphene oxide/carbon nanotube (G/M@SACNT) interlayer with a thickness of 2 μm and an areal density of 0.104 mg cm^{-2} was introduced into the battery system (Figure 7d).[57] Apart from the chemisorption of MnO_2 and skeleton of SACNT films, the graphene oxides can further physically suppress the shuttle of polysulfides. Taking advantages of the synergetic effects of G/M@SACNT interlayer, the binder-free S/SACNT cathode showed an excellent cycling performance with a low capacity decay of 0.029% per cycle at 1 C and high rate performance of 747 mAh g^{-1} at 10 C (Figure 7e), and the shuttle factor was as low as 0.036 after inserting the G/M@SACNT interlayer. A thinner (thickness 1.5 μm) and lighter (areal density 0.087 mg cm^{-2}) interlayer based on the SACNT skeleton with HfO_2 ALD coating was also prepared.[58] After inserting the HfO_2/SACNT film, the cathode delivered a reversible capacity of 836 mAh g^{-1} at 0.2 C based on the weight of the whole electrode, including the interlayer.

5. Flexible Full Cells with Macroscopic SACNT Structures

The 1D feature with excellent flexibility of CNTs provides apparent advantages for manufacturing flexible energy devices, and considerable amount of work has been reported, such as fiber batteries based on CNT/active materials composites.[59,60] As illustrated above, various types of electrodes were manufactured based on the macroscopic structures derived from SACNT arrays, and excellent electrochemical performances were achieved using half-cell tests. It is reasonable to fabricate flexible full cell based on these macroscopic SACNT structures, considering the purpose for potential commercialization and wearable devices. Here, two types of flexible full cells were developed to evaluate the SACNT-based electrodes: (i) pouch cell with Al films and other polymeric materials and (ii) stretchable cell with polymer-based materials.

A pouch cell packed with Al-plastic films consisting of $LiFePO_4$/SACNT cathode, $Li_4Ti_5O_{12}$/SACNT anode, polypropylene separator, and liquid carbonate electrolyte was assembled, as illustrated in **Figure 8**a.[61] The binder-free electrodes were fabricated by spraying the dispersion of active materials onto cross-stacked SACNT films, and the thickness of the electrode can be tuned by repeating the spray-painting and SACNT film cross-stacking steps. At an areal current density of 100 μA cm^{-2}, the narrow gap between voltage plateaus at 1.90 and 1.82 V indicated a slight polarization, which benefited from the excellent ionic diffusion and electronic conductivity provided by the SACNT network. After 30 cycles, the pouch cell delivered an areal capacity of 202 μAh cm^{-2}, corresponding to about 60 mAh g^{-1} based on the total mass of electrodes and separator. After 180° bending, the pouch cell still showed a specific capacity of over 200 μAh cm^{-2}, indicating its high flexibility and strong mechanical robustness of the SACNT scaffold. A full cell consisting of $LiMn_2O_4$/SACNT cathode and TiO_2/SACNT anode was also assembled with polyethylene films through a heat-sealing method.[40] The full cell exhibited an impressive rate performance. At current densities of 5, 10, 20, 30, and 60 C, the cell showed discharge capacities of 150, 120, 95, 80, and 50 mAh g^{-1}. The bending characteristic was also tested. After 500 cycles under bending condition, the cell

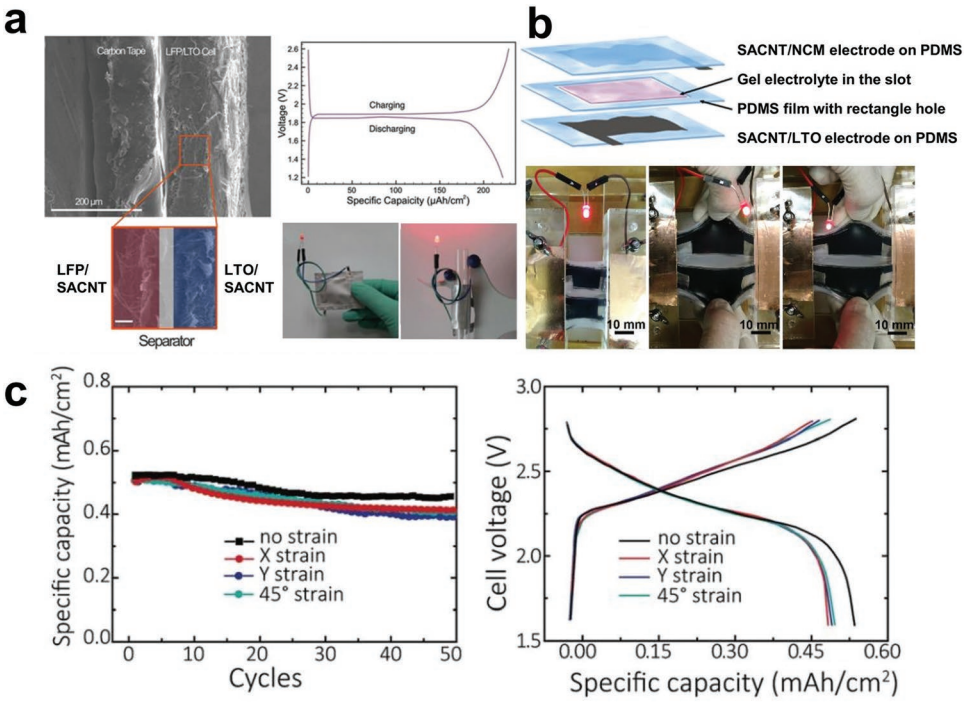

Figure 8. a) SEM images of the LFP/LTO electrode and the optical images and electrochemical performance of the corresponding full cell. Reproduced with permission.[61] Copyright 2014, The Royal Society of Chemistry. b) Schematic and optical images and c) cyclic performance of a full stretchable battery. Reproduced with permission.[64] Copyright 2018, The Royal Society of Chemistry.

still revealed about 80% capacity retention, which was almost the same as the unbent cell.

To match the soft and elastic biological tissues, wearable LIBs should be not only flexible but also stretchable in different directions. Buckled carbonaceous structures are mostly used nanomaterials to design stretchable electronics. Kim and co-workers designed a laterally combed CNTs structure stretchable storage devices.[62] Under the strain of 30%, the stretchable LIBs could power a commercial light-emitting diode. Peng and co-workers reported a novel arch-structured stretchable LIBs, which could maintain a remarkable electrochemical performance at a strain of 400%.[63] However, most of these stretchable LIBs could only sustain decent performance under the deformation in one direction. Ultrastretchable $Li(Ni_{1/3}Co_{1/3}Mn_{1/3})O_2$/CNT and $Li_4Ti_5O_{12}$/CNT electrodes with polydimethylsiloxane substrates were prepared (Figure 8b) that demonstrated excellent electrochemical properties at large strain in different directions.[64] After releasing the prestrain, wrinkled structures form within the composite electrodes and extend along the strain axis to protect the electrode structures from fracture. After 150% strain in different axes, the electrodes showed excellent electrochemical performance, including stable cyclic performance and resistance changes. After assembling with gel electrolyte, the full cell delivered an areal capacity of 0.47 mAh cm^{-2} after 50 cycles with a capacity retention of 90.3%. After 150% strain in the *X*, *Y*, and 45° axes, the full cell showed discharged capacities of 0.41, 0.37, and 0.40 mAh cm^{-2} (Figure 8c). After 2000 tensile cycles, the full cell still exhibited discharged capacities of 0.47, 0.49, and 0.50 mAh cm^{-2}, which demonstrated the ultrastretchability of the full batteries.

6. Summary and Prospects

In the past two decades, energy devices and nanomaterials have become two of the most active research fields, since they are regarded as promising routes toward solving some severe issues of human beings, including energy shortcut and environmental pollution. Even though numerous novel nanomaterials with outstanding properties have been developed, their influence on practical energy devices is still quite limited. One essential problem of this phenomenon is that the unique properties of nanomaterials can hardly be maintained during the construction of macroscopic architectures. SACNTs pave feasible avenues for assembling macroscale CNT devices, since these highly oriented nanotubes can easily constitute continuous structures through their strong intertube force. As summarized in **Table 2**, various formats of macroscopic SACNT architectures have been constructed, including highly oriented thin films, buckypapers, and aerogels. These SACNT architectures have been utilized to form several components in lithium batteries, including composite electrode, current collector, and functional interlayers. A series of lithium batteries containing SACNT-based components have been fabricated, and exhibited excellent electrochemical performance in both half-cell and full-cell tests. These promotions in cell performance can be ascribed to the several advantages of SACNTs and their macroscopic architectures: (i) the high intrinsic conductivity of SACNTs that can provide efficient conductive pathways for electrochemical reaction, (ii) the excellent mechanical properties that can maintain the structural integrity and buffer the volumetric change of electrodes, (iii) the highly oriented nature that

Table 2. Applications of SACNTs for lithium batteries.

Macroscopic structures	Components	Examples (methods)	Electrochemical performance
Highly oriented films	Current collectors	Graphite electrode[48] (traditional slurry casting)	332 mAh g^{-1} at 0.1 C after 50 cycles (180% and 30% improvements in gravimetric and volumetric energy densities)
	Functional interlayers for lithium–sulfur batteries	Pure CNTs[53] G/M@CNT[57] MoS_2/CNT[55] MoP_2/CNT[56] HfO_2@CNT[58]	G/M@MnO_2 interlayer (2 µm): 747 mAh g^{-1} at 10 C HfO_2@CNT interlayer (1.5 µm): 836 mAh g^{-1} at 0.2 C
	Composite electrodes (conducting agents, and current collectors)	$LiCoO_2$[21] (mechanical method) Mn_3O_4, Co_3O_4[35,36] (solution method) Fe_3O_4[37] (magnetron sputtering) NCM/$Li_4Ti_5O_{12}$[64] (spray-painting) $LiFePO_4$/$Li_4Ti_5O_{12}$[61] (spray-painting)	$LiCoO_2$–2 wt% Super P-CNT: 109.6 mAh g^{-1} at 10 C Fe_3O_4–CNT: over 800 mAh g^{-1} at 0.1 A g^{-1} after 100 cycles $LiFePO_4$/$Li_4Ti_5O_{12}$: 202 µ Ah cm^{-2} after 30 cycles
Buckypapers	Composite electrodes (conducting agents, and current collectors)	LTO@CNT[33] (solution methods) MnO_2, and TiO_2[38,39] (solution methods) $LiCoO_2$ (USCD)[18] S(CNT&Air–CNT&CO_2–CNT)[23,27,28] (solution methods)	LTO@CNT: 165.5 mAh g^{-1} after 400 cycles at 1 C MnO_2/aCNT: 630.2 mAh g^{-1} at 2 A g^{-1} after 150 cycles $LiCoO_2$–CNT: 151.4 mAh g^{-1} at 0.1 C after 50 cycles S-CNT: 879 mAh g^{-1} at 10 C
Aerogels	Composite electrodes (conducting agents, and current collectors)	TMO/CNT[40] (solution method)	844, 687, 808, and 902 mAh g^{-1} at 2 A g^{-1} for NiO/CNT, Fe_2O_3/CNT, CO_3O_4/CNT, and MnO_2/CNT electrodes

facilitates sufficient dispersion and full utilization of SACNTs, (iv) the good wettability to electrolyte that is feasible for lithium ions diffusion. The extremely lightweight characteristics of SACNTs make significant contributions to lighten the inert component in the batteries, and gravimetric energy density can be effectively improved. Meanwhile, the highly ordered alignment of SACNTs is beneficial to realize much dense packing than ordinary CNTs, and volumetric energy density can also be increased.

In order to promote the practical applications of SACNTs in advanced lithium batteries, some further work needs to be carried out. From economic point of view, the costly price of CNTs and other novel carbon nanomaterials is still another important restraint of their commercialization. The highly parallel alignment of SACNT can reduce their weight ratio in batteries through sufficient dispersion and full utilization. But the cost by now is still not competitive for the purpose of industry products, which asks for the development of advanced production and processing technology as well as corresponding equipment. Besides, there still exists space for further improvement on the properties of macroscopic SACNT architectures. Considering the neighboring nanotubes are connected by van der Waals force, the SACNT junctions are the bottleneck for the performance such as mechanical strength and thermal conductivity. Strengthening this intertube connection might be a breakthrough toward even better performance for the macroscopic architectures. In addition, there are still plenty of energy devices with macroscopic SACNT structures that remain to be investigated. In the future, macroscopic SACNT architectures can be promoted to other types of lithium batteries, such as the commercially available Si/C anodes and NCM cathodes, even to the Li–air batteries systems. Also, beyond the lithium battery, the application of SACNTs into sodium, magnesium, and zinc batteries can be further explored.

Acknowledgements

Y.F.L. and K.W. contributed equally to this work. This work was supported by the National Natural Science Foundation of China (Grant Nos. 51872158 and 51532008) and the Fundamental Research Funds for the Central Universities (53200759083).

Conflict of Interest

The authors declare no conflict of interest.

Keywords

lithium batteries, macroscopic architectures, superaligned carbon nanotubes

Received: May 26, 2019
Revised: August 30, 2019
Published online: September 29, 2019

[1] J. M. Tarascon, M. Armand, *Nature* **2001**, *414*, 359.
[2] M. Armand, J. M. Tarascon, *Nature* **2008**, *451*, 652.
[3] B. Dunn, H. Kamath, J. M. Tarascon, *Science* **2011**, *334*, 928.
[4] B. A. Johnson, R. E. White, *J. Power Sources* **1998**, *70*, 48.
[5] Z. W. Pan, S. S. Xie, B. H. Chang, C. Y. Wang, L. Lu, W. Liu, M. Y. Zhou, W. Z. Li, *Nature* **1998**, *394*, 631.
[6] R. F. Zhang, Y. Y. Zhang, Q. Zhang, H. H. Xie, W. Z. Qian, F. Wei, *ACS Nano* **2013**, *7*, 6156.
[7] K. L. Jiang, Q. Q. Li, S. S. Fan, *Nature* **2002**, *419*, 801.
[8] K. Liu, Y. H. Sun, L. Chen, C. Feng, X. F. Feng, K. L. Jiang, Y. G. Zhao, S. S. Fan, *Nano Lett.* **2008**, *8*, 700.
[9] K. L. Jiang, J. P. Wang, Q. Q. Li, L. Liu, C. H. Liu, S. S. Fan, *Adv. Mater.* **2011**, *23*, 1154.
[10] U. Dettlaff-Weglikowska, J. Yoshida, N. Sato, S. Roth, *J. Power Sources* **2011**, *158*, A174.
[11] K. Sheem, Y. H. Lee, H. S. Lim, *J. Power Sources* **2006**, *158*, 1425.
[12] X. L. Li, F. Y. Kang, X. D. Bai, W. Shen, *Electrochem. Commun.* **2007**, *9*, 663.
[13] X. M. Liu, Z. D. Huang, S. Oh, P. C. Ma, P. C. H. Chan, G. K. Vedam, K. Kang, J. K. Kim, *J. Power Sources* **2010**, *195*, 4290.
[14] Y. Q. Qian, J. P. Tu, Y. J. Mai, L. J. Cheng, X. L. Wang, C. D. Gu, *J. Alloys Compd.* **2011**, *509*, 10121.
[15] H. Tukamoto, A. R. West, *J. Electrochem. Soc.* **1997**, *144*, 3164.
[16] Y. Shimakawa, T. Numata, J. Tabuchi, *J. Solid State Chem.* **1997**, *131*, 138.
[17] P. S. Herle, B. Ellis, N. Coombs, L. F. Nazar, *Nat. Mater.* **2004**, *3*, 147.
[18] S. Luo, K. Wang, J. P. Wang, K. L. Jiang, Q. Q. Li, S. S. Fan, *Adv. Mater.* **2012**, *24*, 2294.
[19] K. Wang, Y. Wu, S. Luo, X. F. He, J. P. Wang, K. L. Jiang, S. S. Fan, *J. Power Sources* **2013**, *233*, 209.
[20] J. H. Park, S. Y. Lee, J. H. Kim, S. Ahn, J. S. Park, Y. U. Jeong, *J. Solid State Electrochem.* **2010**, *14*, 593.
[21] L. J. Yan, K. Wang, S. Luo, H. C. Wu, Y. F. Luo, Y. Yu, K. L. Jiang, Q. Q. Li, S. S. Fan, J. P. Wang, *J. Mater. Chem. A* **2017**, *5*, 4047.
[22] P. G. Bruce, S. A. Freunberger, L. J. Hardwick, J. M. Tarascon, *Nat. Mater.* **2012**, *11*, 19.
[23] L. Sun, M. Y. Li, Y. Jiang, W. B. Kong, K. L. Jiang, J. P. Wang, S. S. Fan, *Nano Lett.* **2014**, *14*, 4044.
[24] L. Sun, W. B. Kong, Y. Jiang, H. C. Wu, K. L. Jiang, J. P. Wang, S. S. Fan, *J. Mater. Chem. A* **2015**, *3*, 5305.
[25] S. S. Zhang, *Inorg. Chem. Front.* **2015**, *2*, 1059.
[26] T. Z. Hou, X. Chen, H. J. Peng, J. Q. Huang, B. Q. Li, Q. Zhang, B. Li, *Small* **2016**, *12*, 3283.
[27] L. Sun, D. T. Wang, Y. F. Luo, K. Wang, W. B. Kong, Y. Wu, L. N. Zhang, K. L. Jiang, Q. Q. Li, Y. H. Zhang, J. P. Wang, S. S. Fan, *ACS Nano* **2016**, *10*, 1300.
[28] D. T. Wang, K. Wang, H. C. Wu, Y. F. Luo, L. Sun, Y. X. Zhao, J. Wang, L. J. Jia, K. L. Jiang, Q. Q. Li, S. S. Fan, J. P. Wang, *Carbon* **2018**, *132*, 370.
[29] X. L. Ji, K. T. Lee, L. F. Nazar, *Nat. Mater.* **2009**, *8*, 500.
[30] W. B. Kong, L. Sun, Y. Wu, K. L. Jiang, Q. Q. Li, J. P. Wang, S. S. Fan, *Carbon* **2016**, *96*, 1053.
[31] R. Schmuch, R. Wagner, G. Horpel, T. Placke, M. Winter, *Nat. Energy* **2018**, *3*, 267.
[32] G. Xu, P. Han, S. Dong, H. Liu, G. Cui, L. Chen, *Coord. Chem. Rev.* **2017**, *343*, 139.
[33] L. Sun, W. B. Kong, H. C. Wu, Y. Wu, D. T. Wang, F. Zhao, K. L. Jiang, Q. Q. Li, J. P. Wang, S. S. Fan, *Nanoscale* **2016**, *8*, 617.
[34] M. B. Zheng, H. Tang, L. L. Li, Q. Hu, L. Zhang, H. G. Xue, H. Pang, *Adv. Sci.* **2018**, *5*, 1700592.
[35] S. Luo, H. C. Wu, Y. Wu, K. L. Jiang, J. P. Wang, S. S. Fan, *J. Power Sources* **2014**, *249*, 463.
[36] X. F. He, Y. Wu, F. Zhao, J. P. Wang, S. S. Fan, *J. Mater. Chem. A* **2013**, *1*, 11121.
[37] Y. Wu, Y. Wei, J. P. Wang, K. L. Jiang, S. S. Fan, *Nano Lett.* **2013**, *13*, 818.
[38] D. T. Wang, K. Wang, L. Sun, H. C. Wu, J. Wang, Y. X. Zhao, L. J. Yan, Y. F. Luo, K. L. Jiang, Q. Q. Li, S. S. Fan, J. Li, J. P. Wang, *Carbon* **2018**, *139*, 145.
[39] K. L. Zhu, Y. F. Luo, F. Zhao, J. W. Hou, X. W. Wang, H. Ma, H. Wu, Y. G. Zhang, K. L. Jiang, S. S. Fan, J. P. Wang, K. Liu, *ACS Sustainable Chem. Eng.* **2018**, *6*, 3426.
[40] Y. F. Luo, K. Wang, F. Zhao, H. C. Wu, K. L. Jiang, Q. Q. Li, S. S. Fan, J. P. Wang, *ACS Appl. Nano Mater.* **2018**, *1*, 2997.
[41] X. L. Ren, P. C. Lian, D. L. Xie, Y. Yang, Y. Mei, X. R. Huang, Z. R. Wang, X. T. Yin, *J. Mater. Sci.* **2017**, *52*, 10364.
[42] Y. F. Luo, H. C. Wu, L. Liu, Q. Q. Li, K. L. Jiang, S. S. Fan, J. Li, J. P. Wang, *ACS Appl. Mater. Interfaces* **2018**, *10*, 36058.
[43] H. Gwon, H. S. Kim, K. U. Lee, D. H. Seo, Y. C. Park, Y. S. Lee, B. T. Ahn, L. K. Kang, *Energy Environ. Sci.* **2011**, *4*, 1277.
[44] N. Li, Z. P. Chen, W. C. Ren, F. Li, H. M. Cheng, *Proc. Natl. Acad. Sci. USA* **2012**, *109*, 17360.
[45] L. B. Hu, H. Wu, F. L. Mantia, Y. Yang, Y. Cui, *ACS Nano* **2010**, *4*, 5843.
[46] S. Yehezkel, M. Auinata, N. Sezin, D Starosvetskya, Y. Ein-Eli, *J. Power Sources* **2016**, *312*, 109.
[47] S. Yehezkel, M. Auinata, N. Sezin, D Starosvetskya, Y. Ein-Eli, *Electrochim. Acta* **2017**, *229*, 404.
[48] S. K. Martha, J. O. Kiggans, J. Nanda, N. J. Dudney, *J. Electrochem. Soc.* **2011**, *158*, A1060.
[49] C. Arbizzani, S. Beninati, A. Lazzari, M. Mastragotino, *J. Power Sources* **2006**, *158*, 635.
[50] K. Wang, S. Luo, Y. Wu, X. F. He, F. Zhao, J. P. Wang, K. L. Jiang, S. S. Fan, *Adv. Funct. Mater.* **2013**, *23*, 846.
[51] K. Wang, Y. Wu, H. C. Wu, Y. F. Luo, D. T. Wang, K. L. Jiang, Q. Q. Li, Y. D. Li, S. S. Fan, J. P. Wang, *J. Power Sources* **2017**, *351*, 160.
[52] J. Q. Huang, Y. Z. Sun, Y. F. Wang, Q. Zhang, *Acta Chim. Sin.* **2017**, *75*, 173.
[53] L. Sun, W. B. Kong, M. Y. Li, H. C. Wu, K. L. Jiang, Q. Q. Li, Y. H. Zhang, J. P. Wang, S. S. Fan, *Nanotechnology* **2016**, *27*, 075401.
[54] D. H. Liu, C. Zhang, G. M. Zhou, W. Lv, G. W. Ling, L. J. Zhi, Q. H. Yang, *Adv. Sci.* **2018**, *5*, 1700270.
[55] L. J. Yan, N. N. Luo, W. B. Kong, S. Luo, H. C. Wu, K. L. Jiang, Q. Q. Li, S. S. Fan, W. H. Duan, J. P. Wang, *J. Power Sources* **2018**, *389*, 169.
[56] Y. F. Luo, N. N. Luo, W. B. Kong, H. C. Wu, K. Wang, S. S. Fan, W. H. Duan, J. P. Wang, *Small* **2018**, *14*, 1702853.
[57] W. B. Kong, L. J. Yan, Y. F. Luo, D. T. Wang, K. L. Jiang, Q. Q. Li, S. S. Fan, J. P. Wang, *Adv. Funct. Mater.* **2017**, *27*, 1606663.
[58] W. B. Kong, D. T. Wang, L. J. Yan, Y. F. Luo, K. L. Jiang, Q. Q. Li, L. Zhang, S. G. Lu, S. S. Fan, J. Li, J. P. Wang, *Carbon* **2018**, *139*, 896.
[59] Y. Zhang, Y. H. Wang, L. Wang, C. M. Lo, Y. Zhao, Y. D. Jiao, G. F. Zheng, H. S. Peng, *J. Mater. Chem. A* **2016**, *4*, 9002.
[60] H. J. Lin, W. Weng, J. Ren, L. B. Qiu, Z. T. Zhang, P. N. Chen, X. L. Chen, J. Deng, Y. G. Wang, H. S. Peng, *Adv. Mater.* **2014**, *26*, 1217.
[61] Y. Wu, H. C. Wu, S. Luo, K. Wang, F. Zhao, Y. Wei, P. Liu, K. L. Jiang, J. P. Wang, S. S. Fan, *RSC Adv.* **2014**, *4*, 20010.
[62] S. Hong, J. Lee, K. Do, M. Lee, J. H. Kim, S. Lee, D. -H. Kim, *Adv. Funct. Mater.* **2017**, *27*, 1704353.
[63] W. Weng, Q. Sun, Y. Zhang, S. S He, Q. Q. Wu, J. Deng, X. Fang, G. Z. Guan, J. Ren, H. S. Peng, *Adv. Mater.* **2014**, *27*, 1405127.
[64] Y. Yu, Y. F. Luo, H. C. Wu, K. L. Jiang, Q. Q. Li, S. S. Fan, J. Li, J. P. Wang, *Nanoscale* **2018**, *10*, 19972.